Journal of Agroforestry and Environment
Volume 19, Issue 1, 2026

Journal DOI: https://doi.org/10.55706/jae
Journal homepage: www.jagroforenviron.com

Linking Land Use Change to Surface Temperature and Thermal Discomfort: Evidence from Mymensingh, Bangladesh

Ananya Roy[1*], Syeda Tasnim Nowshin[1], Marufa Jahan Tonni[1], Md Habibur Rahman Habib[1] and Mst. Tanjina Akter[1]

[1]Department of Environmental Science and Engineering, Jatiya Kabi Kazi Nazrul Islam University, Trishal, Mymensingh-2224

*Correspondence: ananyaroy058@gmail.com; Mobile: +8801788933294

Received: 24/02/2026
Accepted: 30/05/2026
Available online: 04/06/2026

Abstract: Rapid unplanned urbanization, particularly in developing countries, significantly alters land surface characteristics and microclimatic conditions through LULC changes that increase urban surface temperatures, damage vegetation and water bodies, and contribute to ecosystem degradation, climate change, and accelerated global warming. This study evaluates the spatiotemporal relationships among changes in LULC, surface temperature, and the DI in Mymensingh District, Bangladesh. Satellite images were analyzed for the years 2004, 2015, and 2025, along with meteorological data, using GIS and RS techniques. The results show that the proportion of natural bodies is decreasing because of rapid expansion of built-up areas, resulting a sharp rise in surface temperature and higher DI values. The LULC classification achieved satisfactory accuracy, with overall accuracy ranging from 86–90% and Kappa coefficients between 0.82–0.87. From 2004 to 2025, built-up areas increased by approximately 78%, while vegetation cover and water bodies decreased by 10.54% and 82.28%, correspondingly. The year 2015 represented a transitional phase of urban expansion, during which increased vegetation cover contributed to a decrease in average LST from 25.47°C (2004) to 22.73°C. However, by 2025, rapid urbanization increased the average LST to 24.08°C. Discomfort Index analysis revealed that the region was thermally comfortable in 2004, whereas moderate discomfort zones emerged in 2015 and intensified by 2025, when over 53% of the population is projected to experience moderate discomfort and 4.23% extreme discomfort. Rising thermal stress may increase heat-related illnesses, dehydration, cardiovascular risks, sleep disturbances, mental stress, and economic burdens, with children, elderly people, and vulnerable individuals being the most affected.

Keywords: Land Use Land Cover (LULC); Land Surface Temperature (LST); Discomfort Index (DI); Urbanization; Thermal Discomfort

INTRODUCTION

Urbanization driven by rapid population growth transforms natural landscapes into built-up areas, causing significant environmental and climatic changes (Seto et al. 2012). Land cover modification alters surface properties such as albedo, roughness, and evapotranspiration, which directly influence the Earth's energy balance and spatiotemporal distribution of land surface temperature (LST) (Seto et al. 2012; Bahi et al. 2016). Rapid urban expansion increases LST because built-up materials like asphalt, concrete, and metal absorb and retain more solar radiation (Weng 2009; Halder et al. 2025). In contrast, vegetation and water bodies help reduce surface temperature through shading, evaporation, and transpiration processes, thereby regulating the urban thermal environment temperature (Akbari et al. 2001; Gazi et al. 2020; Grimmond Satellite imagery provides an effective approach for analyzing LULC changes and estimating land surface temperature (LST), while temporal land cover modifications significantly influence temperature patterns and human thermal comfort levels (Ahmed et al. 2026; Li et al. 2016; Weng et al. 2004).

Human thermal comfort is strongly influenced by environmental factors such as air temperature, humidity, solar radiation, and wind speed (Coccolo et al. 2016). In tropical and subtropical regions, high temperature combined with elevated humidity intensifies heat stress and reduces human comfort (Moran et al. 2006; Wong et al. 2024). Prolonged exposure to such thermal discomfort can result in dehydration, heat exhaustion, heat stroke, and even death in

extreme situation. Bangladesh, one of the world's most densely populated countries, is experiencing rapid land cover transformation due to increasing urban expansion, particularly in city areas, which significantly alters the local climate and increases vulnerability to heat stress (Requia et al. 2024; Zhao et al. 2020). According to BBS (2022), Mymensingh is the fourth most populated district in Bangladesh, with a population growth rate of 1.3%. The city's population has doubled since 1981, leading to substantial changes in natural land cover since the 1980s (Rahman et al. 2025; Ahmed et al. 2026). Landsat satellite imagery, available for Mymensingh since 1989, provides an effective source for analyzing long-term LULC and land surface temperature (LST) changes (Jahan 2007; Rakib et al. 2020).

Many studies have been undertaken on a global scale to analyze the relationship between LULC and LST using GIS and Remote Sensing techniques, with multi-temporal satellite imageries (Ahmed et al. 2013; Delina et al. 2024; Dewan and Corner 2013; Gazi et al. 2020; Halder et al. 2025; Kayet et al. 2016; Bokaie et al. 2016; Abdulla-Al Kafy et al. 2020; Maduako et al. 2016; Nguyen et al. 2023; Sourav et al. 2025; Ullah et al. 2023; Ziaul and Pal 2017; Zhao et al. 2020). In Bangladesh, various researchers have found that urbanization leads to significant changes in surface temperatures, leading to the development of urban heat island (Ahmed et al. 2013; Satyanarayana et al. 2020). These researches carried out in Chittagong, Rajshahi, Dhaka, and Barishal city and found considerable growth in built-up surfaces over the past decades that led to an increase in land surface temperatures and further found that the removal of vegetation and degradation of wetlands are responsible for rising temperatures in these city (Abdullah et al. 2022; Ahmed et al. 2013; Hasan et al. 2022; Fayshal et al. 2025; Imran et al. 2021; Hasan et al. 2025). Some research has also been published on outdoor thermal discomfort analysis based on DI (Dasari et al. 2021; Mutanga et al. 2018; Nurmaya et al. 2022) and concluded that DI increases rapidly with the combination of high temperature and humidity. With an increase in the values of the discomfort index, the levels of discomfort experienced by human increase (Sultana et al. 2019). Analyzing thermal discomfort in Bangladesh experienced an increase in average temperature by 0.13°C/decade and relative humidity by 0.3%/decade during 1961–2020 (Ekra et al. 2024). It was found that 67% of settlement increased from 1993 to 2020 and 0.24˚C LST increased/year in Dhaka as a result thermal discomfort shifted from moderate to strong heat stress (Imran et al. 2021). Talukdar et al. (2019) found that thermal discomfort values had been fluctuated from 2012 to 2016 in Dhaka, Sylhet, and Chittagong cities. Again, the relationship between LULC, LST, and NDVI has been highlighted in various studies (Ullah et al. 2023; Fatemi et al. 2019; Naidu et al. 2023).

Several studies have investigated LULC and LST changes in Mymensingh (Rakib et al. 2020; Chowdhury et al. 2018); limited research has investigated their combined influence on human thermal discomfort over time. Although some studies investigated the combined effect of LULC and LST using various statistical tools to calculate DI. Moreover, insufficient attention has been given to understanding how rapid urbanization and the decline of natural bodies contribute to increasing thermal stress and its potential impacts on public health in Mymensingh city. But in this study the effect of LULC, LST, and DI is investigated for the years of 2004, 2015 and 2025 using GIS and RS techniques, and the thermal discomfort state on humans is assessed, which makes the study unique from other studies. This study also focuses on a growing second-tier district (Mymensingh) instead of metropolitan areas. It links human thermal comfort to specific environmental variables, which is rarely been observed in previous studies in Bangladesh. The core goal of this investigation is to evaluate the effects of LULC change and LST on the thermal stress and to identify emerging heat-risk zones within the research area to provide mitigation strategy to reduce the thermal stress.

MATERIALS AND METHODS

Study Area: Mymensingh district is placed in the north-central part of Bangladesh, about 120 km to distant to Dhaka city (Khan et al., 2018). Geographically this area is mostly low lying alluvial flood plain formed by Brahmaputra river system with slightly elevated Pleistocene terrace in southern Madhupur tract (Haque 2018; Chowdhury et al. 2018). The old Brahmaputra River which was once main course of current Brahmaputra runs on its southeast direction of this district which contribute in hydrology, agriculture and ecology of that area (Alam et al. 2007; Islam et al. 2016). According to BBS (2022), the population of Mymensingh district is 5,899,905 and the area is 4,395.13 km². The

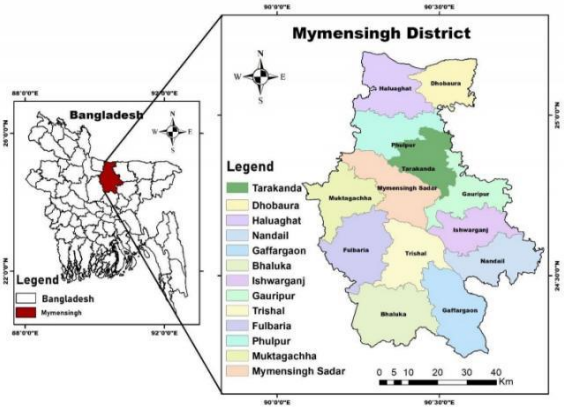

Fig. 1. Study Area Map of Mymensingh District, Bangladesh

climate of Mymensingh district is a monsoon induced moist subtropical climate (Köppen: Cwa). Moderate temperatures, high humidity, and heavy seasonal rainfall are observed. Due to its proximity to the Himalayas, the weather is slightly cooler than the capital Dhaka (Haque 2024). Four seasons exists here, namely winter, summer, monsoon, autumn, characterized by winters (11-25° Celsius) from December to February, summers (23-35° Celsius) from March to May, monsoon (1500-1700 mm annually), which occurs mainly

DOI: https://doi.org/10.55706/jae1915

from June to September, and post-monsoon (150-170 mm annually) from October to November (BMD, 2024). During this time, humidity increase, leading to increased sweating. High humidity and temperatures during the monsoon and pre-monsoon seasons cause significant thermal discomfort, making the area an important focus for climate and urban heat research. Mymensingh city has been undergoing urbanization since the 1980s (Rakib et al. 2020).

Image Preprocessing: The required information is archived from the USGS satellite imagery database, which includes satellite imagery from 2004, 2015, and 2025. Satellite image of 2004 is archived from Landsat 5 TM and of 2015 and 2025 from Landsat 8 OLI/TIRS. The images obtained in this study do not require any further correction, they have been corrected to a first-level terrain corrected product (Ahmed et al. 2013; Bonafoni et al. 2016; USGS 2019). The satellite images obtained are either spectral or thermal (Markham and Barker 2003). Therefore, this study will use satellite images to maintain consistency.

LULC Mapping Using Spectral Bands: Human activities on land are primarily referred to as land use, while land features such as vegetation, water, and soil referred to as land cover (Lambin et al. 2003). The LULC classes were adopted from existing classification systems (Anderson, 1976; Gomarasca, 2009). The stacked images from satellite multispectral data for 2004, 2015 and 2025 are used to categorize the images through the Maximum Likelihood Classifier (MLC). Band combinations are used to improve feature separability and identify suitable samples for classification (Butler 2013; Erener 2013). The accuracy assessment is done by using 200 ground truth samples from MSDP maps, topographic maps, and Google Earth images. The reliability of the classification results is obtained from a confusion matrix (Mahmood et al. 2016; Macarringue et al. 2022)

Derivation of LST: According to Ding and Shi (Shi, 2013), Landsat LST calculated using band 6 of Landsat 5 and band 10 of Landsat 8 using mono-window algorithm. Table 1 includes the information of the Landsat bands. At first, equation (1) was used to transform the digital number (DN) to spectral radiance (L_λ) for thermal bands of Landsat TM and ETM+ whereas equation (2) was employed calculating spectral radiance (L_λ) of Landsat OLI/TIRS. According to Equation (1), the peak atmospheric radiance (L_λ) was calculated in watts for Landsat TM, ETM+, and TIRS bands (USGS 2019).

$$L_\lambda = \left(\frac{L_{MAX}-L_{MIN}}{QCAL_{MAX}-QCAL_{MIN}}\right) \times (QCAL - QCAL_{MIN}) + L_{MIN} \quad (1)$$

Here, L_{MAX} (maximum spectral radiance) = 15.6 (for TM) L_{MIN} (minimum spectral radiance) = 1.238 (for TM), $QCAL_{MAX}$ (maximum DN) = 255, $QCAL_{MIN}$ (minimum DN value) = 1 (Imran et al., 2021),

$$L_\lambda = M_L \times QCAL + A_L \quad (2)$$

where (M_L) denotes the multiplicative rescaling factor (0.0003342), (QCAL) refers to the DN of band 10, and (A_L) indicates the additive rescaling factor (0.1).

Then, following equation (3) converts spectral radiance (L_λ) to satellite brightness temperature T_B (Xulong Duan, 2025)

$$T_B = \frac{k_2}{\ln\left(\frac{k_1}{L_\lambda+1}\right)} \quad (3)$$

Here, K_1 and K_2 are sensor-specific calibration constants.

The LST is estimated by adjusting for emissivity (ε) based on the brightness temperature. Additionally, the emissivity corrected LST was calculated following (Carnahan and Larson 1982; Orimoloye et al. 2016) equation (4). The NDVI values of the image pixels were used to calculate the irradiance, which is dependent on the LULC characteristics.

$$S_T = \frac{T_B}{1+\left(\frac{\lambda T_B}{\rho}\right).\ln \varepsilon} - 273.15 \quad (4)$$

(Sobrino et al., 2004)

Here, (S_T) is LST (°C), λ is the wavelength of emitted radiation = 11.5 μm, ρ = 1.438 × 10^{-2} mK, and ε indicates emissivity explained in equation (5).

$$\varepsilon = 0.004Pv + 0.98 \quad (5)$$

Here, Pv refers to vegetation proportion,

$$Pv = \left(\frac{NDVI-NDVI_{min}}{NDVI_{max}-NDVI_{min}}\right)^2 \quad (6)$$

For Landsat 5, there is no need to calculate emissivity (ε) and P_v (vegetation proportion). Using equations (1) and (3), and then

$$C = K - 273.15 \quad (7)$$

Here, C stands for LST (°C) and K stands for brightness temperature in Kelvin.

Calculation of Human Discomfort Index (DI): Temperature and relative humidity data were acquired from Bangladesh Meteorological organization (BMD), authorized for meteorological data collection. The data are subsequently processed using Microsoft Excel. Explanation of Thom's discomfort index method and calculation of discomfort index were done (Tahir et al. 2013; Assael et al. 2010

$$DI = T_{air} - (0.55 - 0.00RH)(T_{air} - 14.5) \quad (8)$$

Where T_{air} (Air temperature in °C), derived from calibrated LST, average temperature of specific day ($T_{air\,mean}$) and RH or relative humidity (%). T_{air} is calculated using below equation,

$$T_{air} = LST + (T_{air\,mean} - LST_{mean}) \quad (9)$$

Table 1. Thom's discomfort states (Tahir, 2013)

Category	DI Range (°C)	Remark
No Discomfort	<21	No Discomfort
Mild Discomfort	21-25	< 50% of the people feels discomfort
Moderate Discomfort	25-28	>50% of the people feels discomfort

DOI: https://doi.org/10.55706/jae1915

High Discomfort	28-30	Most of the people feels discomfort
Severe Discomfort	30-32	Everyone feels stress
Extreme Heat Stress	>32	State of medical emergency

RESULTS AND DISCUSSIONS

Land Use and Land Cover (LULC) Change Analysis: The LULC maps (Fig. 2) show the changes that have occurred in the Mymensingh District from the year 2004 to 2025. Four main types of land cover have been identified: vegetation, water, bare land, and settlements. In the year 2004, the area under consideration was mostly covered with agricultural land, with forests, settlements, and wetlands. In the year 2015, the area under settlement had increased, while the forest cover and wetlands had decreased. By 2025, settlements had increased, while the agricultural land, forests, and wetlands had decreased.

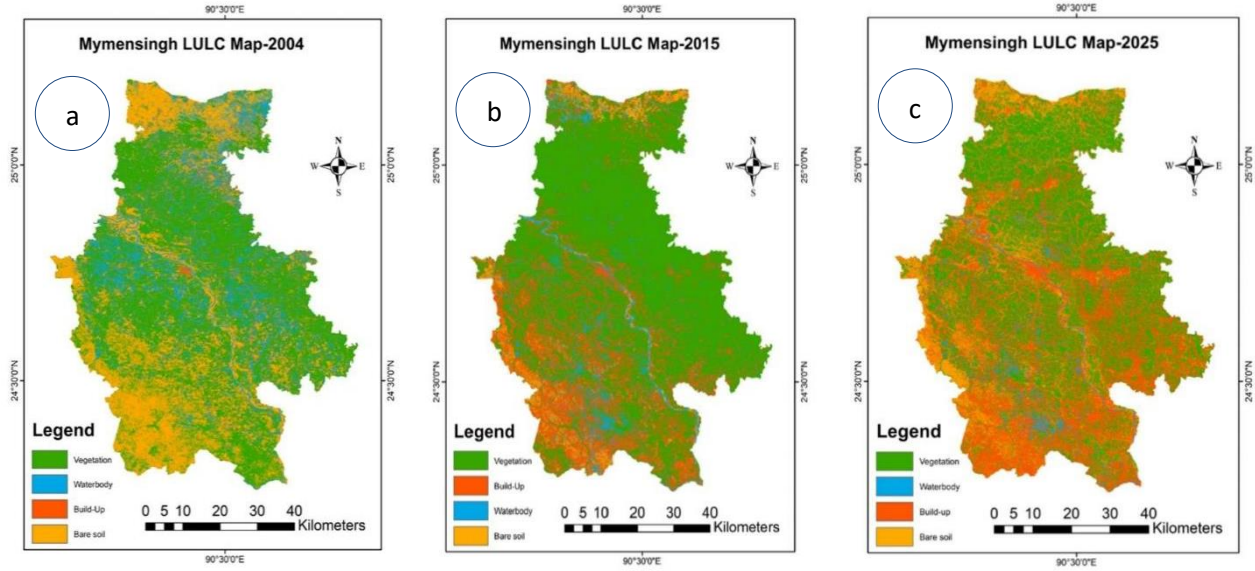

Fig. 2(a) LULC 2004, **(b)** LULC 2015, **(c)** LULC 2025

Table 2. Temporal Change of LULC in Mymensingh (2004-2025)

LULC Class	Area 2004 (km²)	Area 2015 (km²)	Area 2025 (km²)	% Change (2004–2015)	% Change (2015–2025)	% Change (2004–2025)	Overall Trend
Vegetation	2145.77	2806.95	1919.74	+30.82	−31.61	−10.54	Decreased
Water Body	688.67	294.44	122.06	−57.24	−58.55	−82.28	Decreased
Built-up Area	176.82	1045.58	1568.20	+491.32	+49.98	+786.88	Increased
Bare Soil	1337.44	201.79	738.67	−84.91	+266.05	−44.77	Decreased

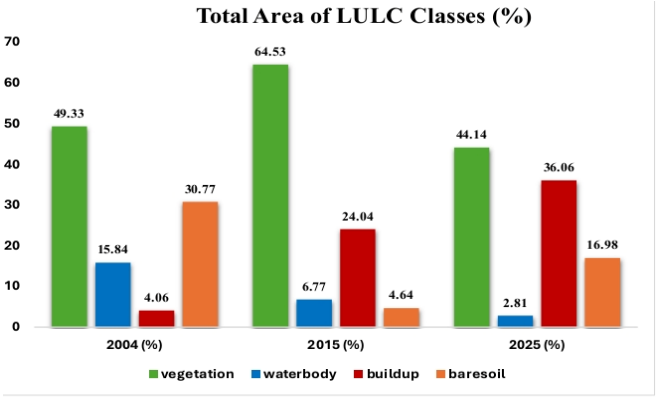

Fig. 3. Percentage Share of Total Land Area for Different LULC Categories (2004 – 2025)

Significant changes are seen in the LULC pattern of Mymensingh district from 2004 to 2025. The vegetation cover of the area was 2145.77 km² in 2004, which increased in the year 2015 to 2806.95 km². But by 2025, the vegetation cover has decreased to 1919.74 km². The expansion in settlement areas in the central and southern sections of the district is the primary cause of land cover change, leading transformation of vegetation and agricultural land into settlement zones. Poor water availability is also evident in this region. The water body cover was initially 688.67 km² in the year 2004, which declined to 294.44 km² in the year 2015 and further declined to 122.06 km² in the year 2025. The extent of settlement areas is increasing in this region. In 2004, the area of settled land was 176.82 km², which increased to 1045.58 km² in 2015 and further to 1568.20 km² in 2025. The bare soil cover is fluctuating in the study area. The bare soil cover was initially 1337.44 km² in the year 2004, declined in.

DOI: https://doi.org/10.55706/jae1915

Accuracy Assessment Results of LULC: The dependability of classified LULC maps for Mymensingh District was checked by accuracy assessment with the help of confusion matrices prepared for the years 2004, 2015, and 2025. The overall Accuracy and Kappa Coefficient values achieved for selected years in the spatiotemporal analysis demonstrated the dependability of the classified results.

From the tables provided, it is evident that the accuracy of LULC classification has progressively improved from 2004 to 2025. Overall accuracy increased from 86.88% in 2004 to 90.63% in 2015 and decreased to 90.25% in 2025, while the user and producer accuracies have been increasing day by day, especially in the built-up and water body categories. The Kappa values for 2004, 2015, and 2025 (0.8254, 0.8750, and 0.850) reveal that the classified results have been highly accurate.

Table 3. Accuracy Assessment for LULC Classification in 2004

Class Value	Vegetation	Water body	Bare soil	Built-up area	Total	User Accuracy	Error of Omission
Vegetation	33	1	3	3	40	82.500	17.5
Water-Body	1	34	3	3	40	85.000	15
Bare soil	1	0	38	1	40	95.000	5
Build-up area	0	0	6	34	40	85.000	15
Total	35	35	50	40	160		
Producer Accuracy	94.286	97.143	76.000	85.000		Kappa Coefficient = 0.8254	
Error of Omission	5.714	2.857	24.000	15.000		Overall Accuracy = 86.875	

Table 4. Accuracy Assessment for LULC Classification in 2015

Class Value	Vegetation	Build-up area	Water Body	Bare soil	Total	User Accuracy	Error of Omission
Vegetation	38	0	1	1	40	95.000	5
Water Body	0	38	1	1	40	95.000	5
Build-up area	4	1	34	1	40	85.000	15
Bare soil	3	1	1	35	40	87.500	12.5
Total	45	40	37	38	160		
Producer Accuracy	84.444	95.00	91.892	92.105		Kappa Coefficient = 0.875	
Error of Omission	15.556	5.000	8.108	7.895		Overall Accuracy = 90.625	

Table 5. Accuracy Assessment for LULC Classification in 2025

Class Value	Vegetation	Water Body	Build-up area	Bare soil	Total	User Accuracy	Error of Omission
Vegetation	32	0	0	8	40	80.000	20
Water Body	1	39	0	0	40	97.500	2.5
Build-up area	0	0	38	2	40	95.000	5
Bare soil	4	0	0	36	40	90.000	10
Total	37	39	38	46	160		
Producer Accuracy	86.487	100.000	100.000	78.261			
Error of Omission	13.514	0.000	0.000	21.7391		Kappa Coefficient = 0.850	
						Overall Accuracy = 90.250	

Spatiotemporal Analysis of Land Surface Temperature (LST): LST maps of Mymensingh District for 2004, 2015, and 2025 (Fig 4) have depicted a spatial variability in the temperature pattern. In the LST map of 2004 (Fig 4a), it was evident that the high LST values were recorded over the urbanized regions and bare soil surfaces, whereas low LST values were recorded over the Brahmaputra.River corridor and wetland regions. In the LST map of 2015 (Fig 4b), a significant cooling trend was recorded over the region, where the major part of the region was covered by low LST values. In the LST map of 2025 (Fig 4c), it was evident that the urban clusters and dry open land surfaces recorded a slight rise in LST values, whereas the Brahmaputra River corridor and vegetation surfaces recorded low LST value.

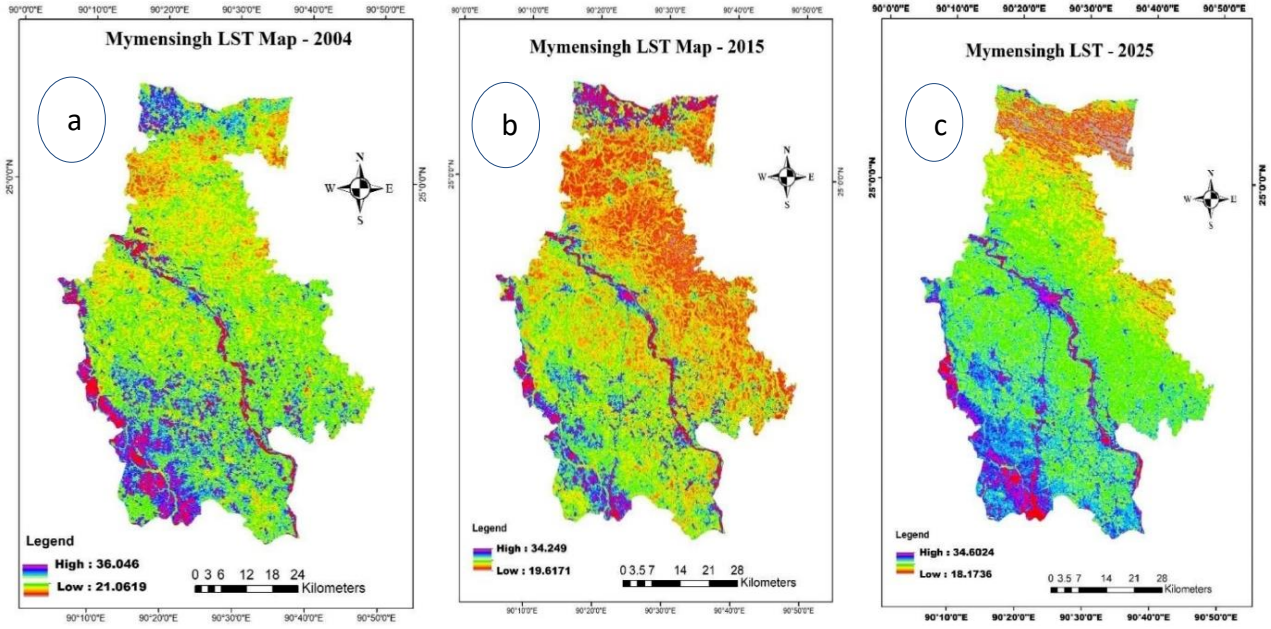

Fig. 1 (a). LST 2004, (b) LST 2015, (c) LST 2025

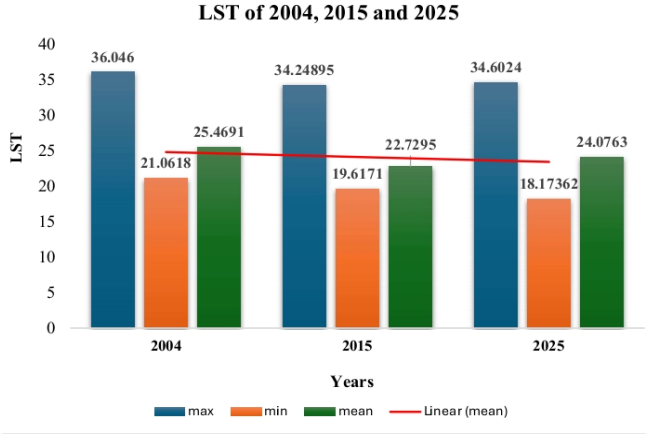

Fig. 2. Trend of LST Mean (2004, 2015, 2025)

It is clear that the district-wide average LST cooled from 26.47 ˚C in 2004 to 22.73˚C in 2015 (reduced to -2.74 °C), and then it warmed up to 24.08 °C in 2025 (+1.35 °C relative to 2015, still 0.39 °C lower than 2004). The maximum LST similarly cooled from 36.05˚C in 2004 to 34.25˚C in 2015 (-1.80˚C), and then it warmed up to 34.60 °C in 2025 (+0.35 °C relative to 2015). In contrast, the minimum LST shows a steady downward trend: 21.06 °C, 19.62 °C, and 18.17 °C. In other words, it cooled steadily over the 2004-2025 period by -2.89 °C. These values suggest that (i) there was a cooling trend over 2004-2015, (ii) follow-up moderate warming, and (iii) widening thermal range driven mainly by colder minima in 2025.

Table 6. Area Percentage of LST

Year	LST Range (ºC)	Category	Approximate Area (%)
2004	21.1-25	Low LST (Cool)	45
	25.1-29.9	Moderate (Transitional)	35
	>30	High LST (Warm)	20
2015	20-24.5	Low LST (Cool Areas)	55
	24.6- 29.9	Moderate (Transitional)	30
	>30	High LST (Warm)	15
2025	20.5-25	Low LST (Cool Areas)	25
	25.1-29.9	Moderate (Transitional)	35
	>30	High LST (Warm Areas)	40

Table 6 depicts the distribution of LST over Mymensingh District during 2004, 2015, and 2025. The distribution is classified into three types of LSTs, namely, Low LST or Cool, Moderate or Transitional, and High LST or Warm. The distribution of LST over Mymensingh District during 2004 revealed that 45% of the area was covered by low LST or cool. The area covered by moderate LST was 35%, while the area covered by high LST or warm was 20%. During 2015, however, the area covered by low LST or cool increased to 55%, while the area covered by moderate LST decreased slightly to 30%, and that covered by high LST or warm decreased to 15%. In 2025, however, the area covered by low LST or cool decreased to 25%, while the area covered by high LST or warm increased to 40%. The area covered by moderate LST remained almost constant at 35%.

DOI: https://doi.org/10.55706/jae1903

Spatiotemporal Analysis of Discomfort Index (DI): The Discomfort Index (DI) maps of Mymensingh District for the years 2004, 2015, and 2025 reveal that the areas in the Mymensingh District have been experiencing increased levels of discomfort over the years.

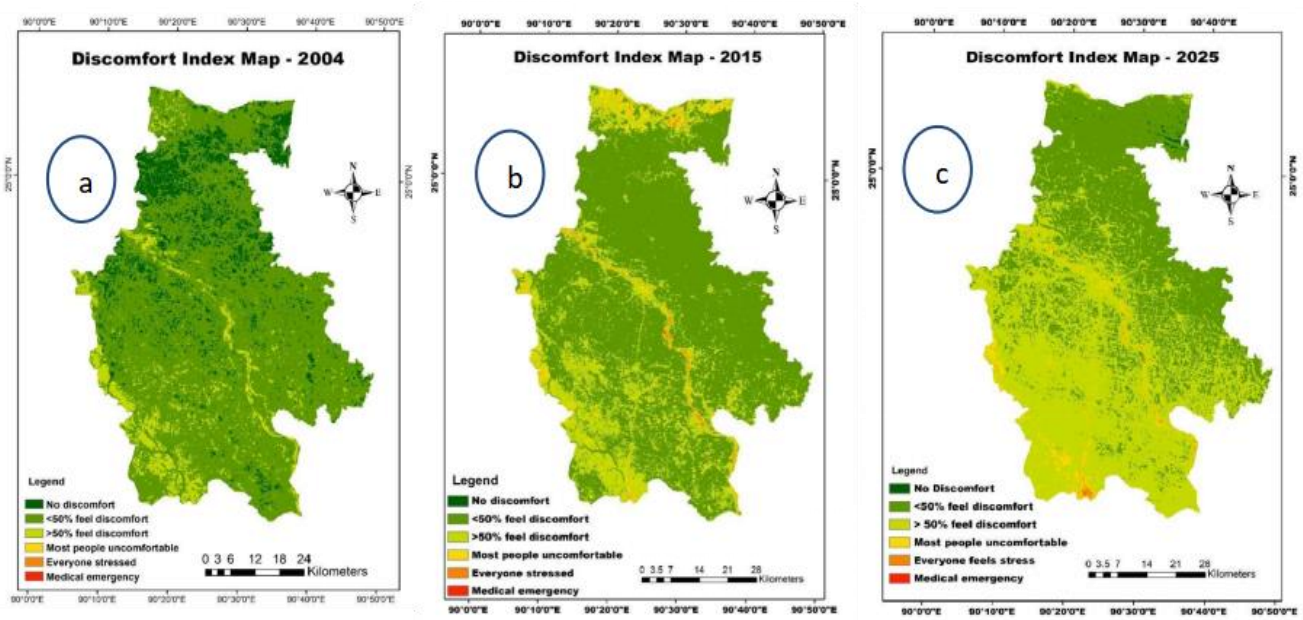

Fig. 6 (a). Discomfort Index 2004, (b) Discomfort Index 2015, (c) Discomfort Index 2025

In the year 2004, most areas in the Mymensingh District were found to have low levels of discomfort, as most areas were covered in green and light-yellow colors. Mild to moderate discomfort are found only the southern and southwestern zone of the map. In 2015, the discomfort index elevated in the southern, central, and eastern portions of the mapped zone, as indicated with yellow and orange colors. In the year 2025, the areas in the southern and southwestern regions were found to have increased in the Discomfort Index maps and were covered in orange and red colors, indicating higher levels of discomfort. The areas in the northern region were found to have low levels of discomfort.

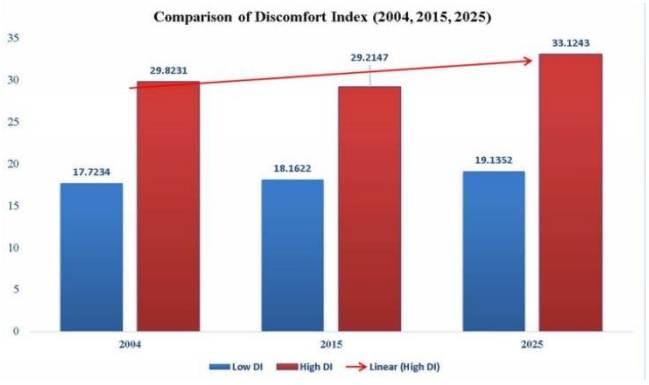

Fig. 7. Comparison of High and Low values of Discomfort Index Over Time (2004, 2015, 2025)

Table 7 and fig. 7, shows the comparison between high and low values of DI in 2004, 2015, and 2025. Besides, fig. 6 displays the spatial pattern of Discomfort Index (DI) in Mymensingh for pre-monsoon 2004, 2015, and 2025. From the pattern, it is evident that there is a trend of increasing, then decreasing, then increasing again in the 21-year period.

Table 7. Discomfort Index of Mymensingh during Early Summer

Category	Remark	2004 (%)	2015 (%)	2025 (%)
No Discomfort	No Discomfort (<21ºC)	9.98	0.00002	0.262
Mild Discomfort	<50% of the Population feels discomfort (21-25 ºC)	57.19	69.46	43.44
Moderate Discomfort	>50% of the Population feels discomfort (25-28 ºC)	32.68	22.69	53.41
High Discomfort	Most of the Population feels discomfort (28-30 ºC)	0.15	3.09	3.53
Severe Discomfort	Everyone feels stress (30-32 ºC)	0.002	0.61	0.65
Extreme Heat Stress	State of medical emergency (>32 ºC)	0	0.02	0.04

From the Discomfort Index (DI) classification, temporal variations in heat stress from 2004 to 2025 are evident. In 2004, 57.19% of the area was between 21 - 24 °C, indicating that less than 50% of people felt uncomfortable, 32.68% of the area was between 25 - 27 °C, and 9.98% was below 21 °C, indicating that they were not uncomfortable. The rate of excess heat requiring medical support was less than 0.2%. In 2015, the number of people experiencing less than 50% discomfort increased to 69.46% of the area and 22.69% of the area experiencing more than 50% discomfort. The effects of heat stress are beginning to be felt in the area. 3.09% of the area is between 28 - 29 °C and 0.61% is between 30 -

DOI: https://doi.org/10.55706/jae1903

32°C. According to the forecasted situation in 2025, the area with more than 50% of people feeling discomfort has increased significantly to 53.41% and the area with less than 50% of people feeling discomfort has decreased to 43.44%, which is a comfortable category. The high-risk area is about 4.23%, which indicates that people in this area are facing higher heat stress, resulting in various physical and psychological problems for the people in the area. Heat exhaustion and heat stroke are heat-related illnesses caused by overheating that can lead to death. It also increases the risk of dehydration, headaches, weakness, high blood pressure and heart disease. Heat also causes sleep problems and mental stress, which reduces human performance and productivity. Children, the elderly and the sick are especially at risk. Therefore, the rise in DI has a significant negative effect on quality of life and public health, while also impacting the local economy due to increasing healthcare expenses.

Relation between LULC, LST, and DI: The integrated analysis of LULC, LST, and DI in study area from 2004 to 2025 revealed strong relationships among LULC changes, surface temperature, and human thermal comfort. Higher LST values were detected where in parts largely dominated by build-up land and bare soil, which ultimately caused greater discomfort in the high-temperature zones (marked by red border in fig. 8, 9 and 10).

In 2004, the area was mostly covered by vegetation and agricultural lands. The mean LST was approximately 25.47 °C. Most areas of the region were under "No Discomfort" or "Under 50% feels Discomfort" classes. Mild discomfort was perceived in southwestern part of Mymensingh, where higher surface temperatures were recorded due to the existing land cover characteristics.

In 2015, built-up areas increased, while water bodies showed a decline in exchange of build-up area and agricultural land indicating increase in vegetated area (Table 4). Although the mean LST was slightly decreased to 22.72 °C, almost no place of that area was felt comfortable in that period. Additionally, DI patterns showed emerging heat stress, where most of the area people feel mild discomfort (approximately 70%), 3.09% of the area experienced high discomfort where "Most of the population in that area experiences discomfort" and 0.61% area was under heat stress where "Everyone feels discomfort."

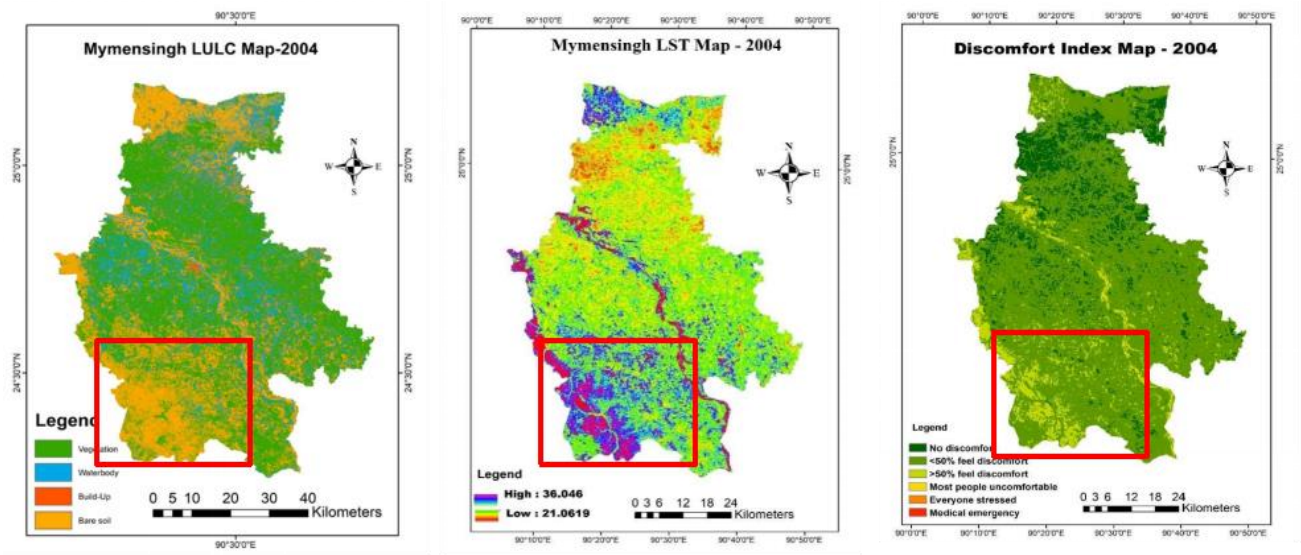

Fig. 8. Relation between LULC, LST and DI in 2004

DOI: https://doi.org/10.55706/jae1903

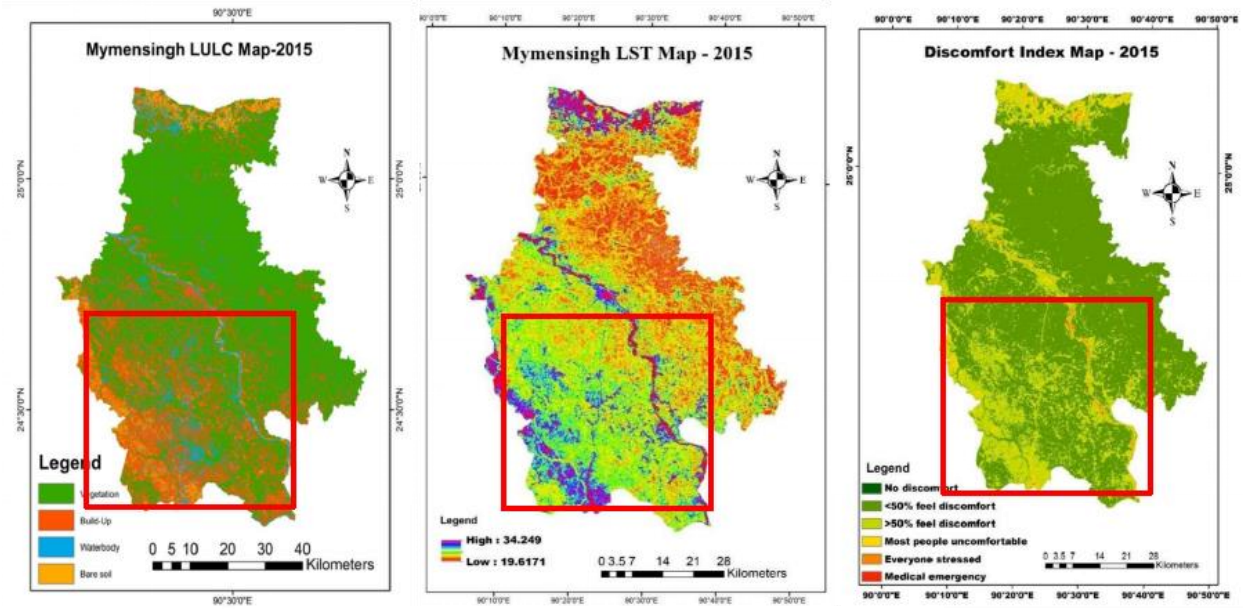

Fig. 9. Relation between LULC, LST and DI in 2015

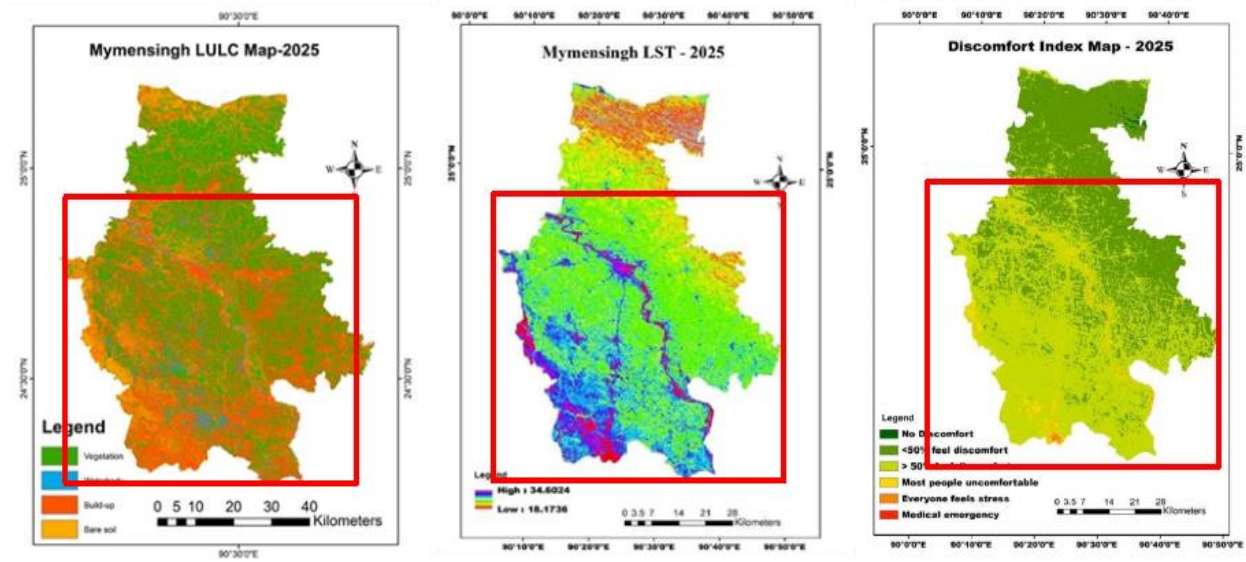

Fig. 10. Relation between LULC, LST and DI in 2004

In 2025, built-up area expansion was maximum over the last 20 years and is evident in fig. 10. Throughout this timeframe, the extent of vegetation and water bodies decreased, while settlements has increased more than 7 times. Moreover, the mean LST increased to 24.08 °C and 40% area experienced high surface temperature which is the highest value compared to previous years. In addition, over 53% of the area people feel moderate heat stress indicating "Over 50% of the population feels discomfort" in the DI category. Worst part is that in few areas situation deteriorated to the medical emergency situation (0.04% of the total area).

LULC changes in Mymensingh district suggest that the region is undergoing rapid urbanization along with growing human pressure on the environment. In 2004, Mymensingh was mostly vegetated and agricultural, with a moderate LST, as well as most of the area falling under the "No Discomfort" to mild discomfort (<50% people feels Discomfort) DI classes. Urban expansion over the decades causing destruction of vegetation, wetland, and agricultural areas, which provides information on the increasing human pressure and population growth in the region (Cartalis et al. 2005; Uddin et al. 2024). The high green cover and surface moisture kept the surface temperature lower, which corroborates previous findings that vegetation reduces heat absorption through evapotranspiration and shading (Kayet et al. 2016; Ziaul and Pal 2017). By 2015, there was evidence of an expansion of settlement areas and a contraction of water bodies. The alteration of natural land cover (vegetation and wetlands) into settlement and open spaces has resulted in a growing prevalence of surfaces with hight heat capacity. That statement was proven as high LST zone (>30°C) in study area have been raised twice within 2 decades. Though

DOI: https://doi.org/10.55706/jae1903

LST mean value slightly decreased to 22.72°C, which can be accountable to seasonal climatic variation and the intensification of agriculture marked during the year 2015, again raised to 24.08°C within 2025. Areas characterized by bare soil and built-up areas, especially in rural areas-Mymensingh Sadar Upazila, Trishal Upazila, and some areas in Bhaluka Upazila, have higher LST due to increased solar radiation and impervious areas. Conversely, vegetation and water serve to cool the surface temperature due to evapotranspiration and moisture retention (Kayet et al. 2016; Ziaul and Pal 2017)

The increase in Discomfort Index (DI) also reflects the increase in thermal stress in the region. The change in the Discomfort Index is associated with the increase in LST, loss of vegetation, and loss of water bodies in the region (Andrade 2008; Makrogiannis et al. 1982). Fig 8, 9 and 10 proves how rapid expansion of build-up area influence surface temperature and ultimately enhance the thermal stress of local residence. Hence, it can be concluded that there is a clear association between urbanization and loss of vegetation, which increases LST, causing an increase in the Discomfort Index and thus reducing human thermal comfort in the region (Faisal et al. 2020).

CONCLUSION

The investigation proves that the alteration in LULC from 2004 to 2025 have affected environmental and thermal conditions of Mymensingh district. The results undoubtedly signpost a substantial escalation in LST and thermal discomfort, mostly driven by quick urban expansion, unplanned land alteration, and the decline of vegetative cover. Settlement areas have expanded significantly, replacing natural land cover has exaggerated the urban temperature and increased the spatial extent of high heat stress zones. The area of vegetation reduced from 2145.77 km² in 2004 to 1919.74 km² in 2025, showing a reduction of -10.54%. Moreover, the area of water body has decreased by -82.28% from 688.67 km² to 122.06 km². In contrast, the inhabited area has increased significantly from 176.82 km^2 to 1568.20 km^2, indicating an increase of 786.88%. In addition, the results of land surface temperature show that the mean LST decreased from 25.47˚C in 2004 to 22.73˚C in the 2015, but increased to 24.08˚C in 2025. And the area of high temperature zone (>30˚C) increased from 20% to 40% in 20 years (2004-2025).

Moreover, the results of the Thermal Discomfort Index (DI) also show that the thermal comfort is deteriorating. The average DI rises from 23.77 in 2004 to 26.13 in 2025, while in the uncomfortable zone (DI = 25-27 °C) rises from 32.68% to 53.41%. Overall, the results show that speedy urban-sprawling, loss of plants, and decrease in water bodies are major contributors to the rise in surface temperature and discomfort.

Overall, the urgent necessity for sustainable land-use practices and climate-responsive urban development in Mymensingh district is the main driving force behind this research. Increasing urban green cover, conserving water bodies, optimizing building layouts, and adopting nature-based solutions are essential to mitigate the increasing heat waves and improve urban livability. The outcome of this research can support policymakers and planners in developing targeted adaptation strategies to promote resilient and thermally comfortable urban environments under ongoing climate change conditions.

Acknowledgements

Gratitude is extended to all data sources (USGS and BMD) and contributors from Environmental Science and Engineering department whose work made this study possible.

Conflict of Interest

The authors stated no potential conflicts of related to this research.

REFERENCES

Ahmed, N.U., Mahmud, N.U., Salim, M., Halder, S.C. and Abdulla-Al Kafy, M., Al Rakib, A.A., Akter, K.S. and Faisal, A.A. 2020. Modelling future land use land cover changes and their impacts on land surface temperatures in Rajshahi, Bangladesh. Remote Sensing Applications: Society and Environment.

Ahmed, A.B., Miah, M.M. and others. 2026. Application of seasonal-adjusted hybrid models for forecasting discomfort index in heat-prone region of Bangladesh. PLOS ONE.

Ahmed, B., Kamruzzaman, M., Zhu, X., Rahman, M.S. and Choi, K. 2013. Simulating land cover changes and their impacts on land surface temperature in Dhaka, Bangladesh. Remote Sensing of Environment, 128: 135–147.

Akbari, H., Pomerantz, M. and Taha, H. 2001. Cool surfaces and shade trees to reduce energy use and improve air quality in urban areas. Solar Energy, 70(3): 295–310.

Alam, J.B., Uddin, M., Ahmed, J.U., Cacovean, H., Rahman, M.H., Banik, B.K. and Yesmin, N. 2007. Study of morphological change of River Old Brahmaputra and its social impacts by remote sensing.

Anderson, J.R., Hardy, E.E., Roach, J.T. and Witmer, R.E. 1976. A land use and land cover classification system for use with remote sensor data. US Government Printing Office, Washington, DC.

Andrade, M.J. 2008. Global warming and the urban heat island. Geographical Bulletin, 53(1): 3–20.

Assael, H., Keivani, A. and others. 2010. Thermal comfort conditions and discomfort index in urban environments. Building and Environment, 45(3): 556–563.

Bahi, H., Rhinane, H., Bensalmia, A., Fehrenbach, U. and Hakdaoui, M. 2016. Impact of urbanization on land use/land cover and surface temperature in Casablanca, Morocco. Remote Sensing, 8(10): 829.

Bangladesh Bureau of Statistics (BBS). 2022. Population and Housing Census 2022: Preliminary Report. BBS, Dhaka.

Bangladesh Meteorological Department (BMD). 2024. Climate of Bangladesh. Bangladesh Meteorological Department, Dhaka.

Bokaie, M., Zarkesh, M.K., Arasteh, P.D. and Hosseini, A. 2016. Assessment of urban heat island based on the relationship between land surface temperature and land use/land cover in Tehran. Sustainable Cities and Society, 28: 94–104.

Brown, B. and Aaron, M. 2001. The politics of nature. In: Smith, J. (ed.) The rise of modern genomics, 3rd edn. Wiley, New York, pp. 230–257.

Butler, T. 2013. Remote sensing for land use analysis. Springer, New York.

Carnahan, D.A. and Larson, R.C. 1982. An analysis of urban heat sink. Remote Sensing of Environment, 12(4): 313–329.

Cartalis, C., Synolakis, C. and Feidas, H. 2005. Daytime urban heat islands from Landsat ETM+ and CORINE land cover data. International Journal of Remote Sensing.

Dewan, A.M. and Corner, R. 2013. Dhaka megacity: Geospatial perspectives on urbanisation, environment and health. Springer, Dordrecht.

Ekra, A.T., Mondal, M.M. and others. 2024. Changes in human heat discomfort and its drivers in Bangladesh. Urban Climate.

Erener, M. 2013. Optimizing spectral bands for land use land cover classification. International Journal of Remote Sensing, 34: 5678–5690.

Faisal, M., Tareq, Y. and others. 2020. Modeling spatio-temporal land transformation and its associated impacts on land surface temperature. Remote Sensing.

Fatemi, M., Narangifard, M. and others. 2019. Monitoring LULC changes and its impact on land surface temperature and NDVI in District 1 of Shiraz City. Arabian Journal of Geosciences.

Gomarasca, M.A. 2009. Land use/land cover classification systems. In: Basics of geomatics. Springer, Dordrecht, pp. 561–598.

Grimmond, S. 2007. Urbanization and global environmental change. Global Environmental Change, 17: 1–3.

Halder, N. and others. 2025. Spatiotemporal assessment of urban thermal discomfort in Kolkata, India: Insights from cloud-based remote sensing. IEEE Journal of Selected Topics in Applied Earth Observations and Remote Sensing, 18.

Hasan, M., Hossain, L. and others. 2022. Urban green space mediates spatiotemporal variation in land surface temperature: A case study of an urbanized city in Bangladesh. Environmental Science and Pollution Research.

Hasan, T., Zhang, J. and others. 2021. Surface urban heat island dynamics in response to land use land cover and vegetation across South Asia. Remote Sensing.

Haque, M.S. 2018. Land use and land cover change analysis using remote sensing and GIS in Mymensingh District of Bangladesh. Journal of Environmental Science and Natural Resources, 11(1–2): 109–116.

Imran, H.M., Hossain, A. and others. 2021. Impact of land cover changes on land surface temperature and human thermal comfort in Dhaka City, Bangladesh. Earth Systems and Environment: 667–693.

Islam, M., Datta, T., Ema, I., Kabir, M. and Meghla, N. 2016. Investigation of water quality from the Brahmaputra River in Sherpur District. Bangladesh Journal of Scientific Research, 28(1): 35–41.

Jahan, M.A. 2007. Urbanization and environmental change in Bangladesh. Journal of Environmental Science and Natural Resources, 1(2): 45–52.

Kayet, N., Pathak, K., Chakrabarty, A. and Sahoo, S. 2016. Spatial impact of land use/land cover change on land surface temperature in an urban area. Sustainable Cities and Society.

Khan, A., Guttormsen, A., & Roll, K. H. (2018). Production risk of pangas (Pangasius hypophthalmus) fish farming. Aquaculture Economics & Management, 22(2), 192–208. https://doi.org/10.1080/13657305.2017.1284941

Lambin, E.F., Geist, H.J. and Lepers, E. 2003. Dynamics of land-use and land-cover change in tropical regions. Annual Review of Environment and Resources, 28: 205–241.

Li, Y., Qian, F., Xi, J. and others. 2016. Research on urban heat-island effect. Procedia Engineering: 11–18

Macarringue, L.S., Liu, E. and others. 2022. Developments in land use and land cover classification techniques in remote sensing: A review. Journal of Geographic Information System: 1–28.

Maduako, I.D., Yunusa, Z. and others. 2016. Simulation and prediction of land surface temperature dynamics within Ikom City in Nigeria using artificial neural network. Journal of Remote Sensing and GIS: 1–7.

Mahmood, R. and others. 2016. Ground truth validation for land use land cover classification. Environmental Monitoring and Assessment, 188: 1–15.

Makrogiannis, I.E. and others. 1982. Heat stress and the human body. Ergonomics, 25(1): 41–48.

Markham, B.L. and Barker, J.L. 2003. Revised Landsat-5 TM radiometric calibration procedures and postcalibration dynamic ranges. IEEE Transactions on Geoscience and Remote Sensing, 41(11): 2674–2677.

Mokarram, M., Taghizadeh-Mehrjardi, R. and others. 2024. Spatial-temporal analysis of atmospheric environment in urban areas using remote sensing and neural networks. Sustainable Computing: Informatics and Systems.

Moran, D.S., Epstein, Y. and others. 2006. Thermal comfort and the heat stress indices. Industrial Health: 135–147.

Murphy, L.S. and Walsh, E.M. 1972. Correction of micronutrient deficiencies with fertilizers. In: Mortvedt, J.J., Giordano, P.M. and Lindsay, W.L. (eds.) Proceedings of Micronutrients in Agriculture. Soil Science Society of America, Wisconsin, USA.

Mutanga, O., Dube, T. and others. 2018. Outdoor thermal discomfort analysis in Harare, Zimbabwe in Southern Africa. South African Geographical Journal.

Naidu, B.N.K., Ahmed, F.A. and others. 2023. Assessing land use land cover changes and land surface temperature through NDVI and NDBI spatial indicators: A case of Bengaluru, India. GeoJournal.

Nguyen, C.T., Chen, A.C. and others. 2023. Urban thermal environment under urban expansion and climate change: A regional perspective from Southeast Asian big cities.

Nurmaya, E.M., Aditya, A.A. and others. 2022. Heat stress analysis using the discomfort index method: Impact on macro-environmental conditions in Yogyakarta. Journal of Ecological Engineering.

Oke, T.R. 1982. The energetic basis of the urban heat island. Quarterly Journal of the Royal Meteorological Society, 108: 1–24.

Oke, T.R. 2003. Thermal remote sensing of urban climates. Remote Sensing of Environment, 86: 370–384.

Orimoloye, I.A., Ololade, O.O. and others. 2018. Land surface temperature and land use land cover dynamics in a rapidly urbanizing region. Environmental Monitoring and Assessment, 190.

Qiantao, Z., Li, Z. and others. 2020. Thermal comfort models and their developments: A review. KeAi.

Rakib, A.A., Sarker, K.S. and others. 2020. Analyzing the pattern of land use land cover change and its impact on land surface temperature: A remote sensing approach in Mymensingh, Bangladesh. Student Research Conference Proceedings.

Rahman, M.M., Sarker, N. and others. 2025. Assessing heat index changes in the context of climate change in Bangladesh. In: Proceedings of International Conference on Civil Engineering Research and Innovations, pp. 12–14.

Rayeen, M.S., Mahmud, T. and others. 2026. Quantifying the impact of land use and land cover change on land surface temperature using spatiotemporal multispectral remote sensing data. Discover Environment, 4(1): 36.

Requia, W.J., Adams, M.D. and others. 2024. Thermal stress and hospital admissions for cardiorespiratory disease in Brazil. Elsevier.

Satyanarayana, M.S. and others. 2020. Urban heat island intensity during winter over metropolitan cities of India. Meteorology and Atmospheric Physics.

Seto, K.C., Güneralp, B. and Hutyra, L.R. 2012. Global forecasts of urban expansion to 2030 and direct impacts on biodiversity and carbon pools. Proceedings of the National Academy of Sciences, 109(40): 16083–16088.

Shi, T., Ding, L. and others. 2013. Land surface temperature retrieval from Landsat data using the mono-window algorithm. Remote Sensing, 5(3): 1444–1460.

Silivia Coccolo, J., Kämpf, J. and others. 2016. Outdoor human comfort and thermal stress: A comprehensive review on models and standards. Elsevier.

Siswanto, M., Rahman, M. and others. 2024. Assessment of surface urban heat island in Indonesia's municipal cities.

Sobrino, J.A., Jiménez-Muñoz, J.C. and Paolini, L. 2004. Land surface temperature retrieval from Landsat TM 5. Remote Sensing of Environment, 90(4): 434–440.

Sourav, K., Rahman, M. and others. 2025. Land cover changes and land surface temperature dynamics in the Rohingya refugee area, Cox's Bazar, Bangladesh: An analysis from 2013 to 2024. Atmosphere, 250.

Sultana, M.S. and others. 2019a. Spatial variability of thermal comfort in Dhaka City. Sustainable Cities and Society, 46: 101–109.

Sultana, M.S. and others. 2019b. Urban land use change and its impact on thermal environment in Bangladesh. Environmental Monitoring and Assessment.

Survey, U.S. 2019. Landsat 7 Data Users Handbook. Sioux Falls, USA.

Tahir, F.Y. and others. 2013. Assessment of thermal discomfort using Thom's discomfort index. International Journal of Environmental Science, 3(2): 123–130.

Talukdar, M.S., Saha, M.S. and others. 2017. Trends of outdoor thermal discomfort in Mymensingh: An application of Thom's discomfort index. Journal of Environmental Science and Natural Resources, 10(2): 151–156.

Talukdar, S.J., Kabir, A.K. and others. 2019. Evaluation of outdoor thermal discomfort of three cities of Bangladesh. In: International Conference on Sustainability in Natural and Built Environment.

Thom, E.C. 1959. The discomfort index. Weatherwise, 12: 57–61.

Tisdale, S.L., Nelson, W.L. and Beaton, J.D. 1982. Soil fertility and fertilizers. Macmillan Publishing Co., New York, pp. 27–35.

United States Geological Survey (USGS). 2019. Landsat 8 Data Users Handbook. Sioux Falls, USA.

Uddin, M.A., Sarker, M.S. and others. 2024. Urban growth-driven land use and climate dynamics: Assessing changes in Dhaka City (1990–2022). Jagannath University Journal of Life and Earth Sciences: 153–177.

Ullah, W., Ahmad, K. and others. 2023. Analysis of the relationship among land surface temperature, land use land cover, and normalized difference vegetation index with topographic elements in the lower Himalayan region. Heliyon.

Vani, M. and Prasad, P.R.C. 2020. Assessment of spatio-temporal changes in land use and land cover, urban sprawl, and land surface temperature in and around Vijayawada City, India. Environment, Development and Sustainability: 3079–3095.

Weng, Q. 2009. Thermal infrared remote sensing for urban climate studies. Remote Sensing of Environment, 113: 1–3.

Weng, Q., Lu, D. and Schubring, J. 2004. Estimation of land surface temperature–vegetation abundance relationship for urban heat island studies. Remote Sensing of Environment, 89: 467–483.

Wong, M.C., Wang, J. and others. 2024. A 1940–2020 spatiotemporal analysis of thermal discomfort days in Southeast Asian countries. Environmental Research Communications, 6(10).

Zhang, X., Wang, D. and others. 2017. Effects of land use/cover changes and urban forest configuration on

urban heat islands in a loess hilly region: A case study based on Yan'an City, China. International Journal of Environmental Research and Public Health.

Zhao, Q., Li, Z. and others. 2020. Thermal comfort models and their developments: A review.

Ziaul, S. and Pal, S. 2017. Detection of land use and land cover change and land surface temperature in English Bazar urban centre. Egyptian Journal of Remote Sensing and Space Science.

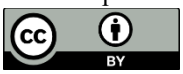

DOI: https://doi.org/10.55706/jae1903